AGU PUBLICATIONS

JGR

Journal of Geophysical Research: Space Physics

RESEARCH ARTICLE
10.1002/2017JA024629

Key Points:
- MAVEN LPW electron density measurements are used to improve the results of MARSIS ionospheric sounding
- LPW and MARSIS electron densities are compared for four coincident events
- There is good agreement between the two data sets; MARSIS electron densities are typically slightly larger

Correspondence to:
F. Němec,
frantisek.nemec@gmail.com

Citation:
Nemec, F., Morgan, D. D., Fowler, C. M., Kopf, A. J., Andersson, L., Gurnett, D. A., Andrews, D. J., & Truhlik, V. (2017). Ionospheric electron densities at Mars: Comparison of Mars Express ionospheric sounding and MAVEN local measurements. *Journal of Geophysical Research: Space Physics*, *122*, 12,393–12,405. https://doi.org/10.1002/2017JA024629

Received 27 JUL 2017
Accepted 8 NOV 2017
Accepted article online 13 NOV 2017
Published online 5 DEC 2017

©2017. American Geophysical Union. All Rights Reserved.

Ionospheric Electron Densities at Mars: Comparison of Mars Express Ionospheric Sounding and MAVEN Local Measurements

F. Němec[1], D. D. Morgan[2], C. M. Fowler[3], A. J. Kopf[2], L. Andersson[3], D. A. Gurnett[2], D. J. Andrews[4], and V. Truhlik[5]

[1]Faculty of Mathematics and Physics, Charles University, Prague, Czech Republic, [2]Department of Physics and Astronomy, University of Iowa, Iowa City, IA, USA, [3]Laboratory for Atmospheric and Space Physics, University of Colorado Boulder, Boulder, CO, USA, [4]Swedish Institute of Space Physics, Uppsala, Sweden, [5]Institute of Atmospheric Physics, Czech Academy of Sciences, Prague, Czech Republic

Abstract We present the first direct comparison of Martian ionospheric electron densities measured by the Mars Advanced Radar for Subsurface and Ionospheric Sounding (MARSIS) topside radar sounder on board the Mars Express spacecraft and by the Langmuir Probe and Waves (LPW) instrument on board the Mars Atmosphere and Volatile Evolution Mission (MAVEN) spacecraft. As low electron densities are not measured by MARSIS due to the low power radiated at low sounding frequencies, MARSIS electron density profiles between the local electron density and the first data point from the ionospheric sounding ($\approx 10^4$ cm^{-3}) rely on an empirical electron density profile shape. We use the LPW electron density measurements to improve this empirical description and thereby the MARSIS-derived electron density profiles. We further analyze four coincident events, where the two instruments were measuring within a 5° solar zenith angle interval within 1 h. The differences between the electron densities measured by the MARSIS and LPW instruments are found to be within a factor of 2 in 90% of measurements. Taking into account the measurement precision and different locations and times of the measurements, these differences are within the estimated uncertainties.

1. Introduction

Electron densities in the Martian ionosphere are now routinely measured both by the Mars Advanced Radar for Subsurface and Ionospheric Sounding (MARSIS) topside radar sounder on board the Mars Express spacecraft and by the Langmuir Probe and Waves (LPW) instrument on board the Mars Atmosphere and Volatile Evolution Mission (MAVEN) spacecraft. The MARSIS data start back in 2005, while the MAVEN data begin in 2014, so there is already a significant overlap of the two missions. Given that the two instruments use completely different physical principles to determine the electron densities, each with its own possible drawbacks, it is of importance to compare the measured electron densities and to identify any possible systematic biases.

Given that electron densities lower than about 10^4 cm^{-3} are usually not detectable by the MARSIS instrument (Němec et al., 2010), we will limit the analysis to the dayside. The electron densities in the dayside ionosphere are controlled primarily by photoionization (Withers, 2009). Two principally different altitudinal regions can be distinguished (Němec et al., 2011). At altitudes close to the peak electron density, the ionosphere is dominated by photochemistry, and the electron density profiles typically follow well the profile shapes predicted by a classical Chapman theory (Chapman, 1931a, 1931b), as documented by, for example, Fox and Yeager (2006), Gurnett et al. (2005, 2008), and Morgan et al. (2008). The Chapman theory also successfully predicts the peak electron density behavior as a function of solar zenith angle (SZA) (Mendillo et al., 2013) and solar irradiance (Girazian & Withers, 2013). At higher altitudes, the plasma transport becomes important. Although the ionospheric structure may be sometimes rather complex (Withers, Fallows, et al., 2012), an exponential decrease of the electron density with altitude is typically observed (Andrews et al., 2013; Duru et al., 2008, 2011). The transition altitude between the two different parts of the profile is typically about 200 km (Ergun et al., 2015; Vogt et al., 2016).

The dayside ionosphere exhibits short-duration/small-scale turbulence-like density fluctuations at timescales on the order of minutes and characteristic spatial correlation scales not more than 20 to 50 km (Gurnett et al., 2010). A mean variation in the peak electron density is found to be about 6% (Wang et al., 2012), and it progressively increases toward higher altitudes, being a few tens of percent at altitudes of about 300 km (Gurnett et al., 2010). However, when limited to altitudes below about 200 km, one may in the first approximation assume that if two spacecraft pass through the same region with a time delay less than a couple of hours, they should observe comparable electron densities. One may possibly even weaken the criteria and require the spacecraft to pass not necessarily through the same region but through the same SZA interval. Considering that the main part of the ionospheric variability is due to the SZA and incoming solar radiation flux, this condition should also ensure a comparable ionospheric situation. It assumes that the dayside ionosphere is not significantly driven by crustal magnetic fields, which is prudent at low altitudes, but no longer completely correct at altitudes above the transition altitude (Andrews et al., 2013; Němec, Morgan, Gurnett, Andrews, 2016).

No direct assessment between the Mars Express/MARSIS radar sounding and MAVEN/LPW electron density measurements has been done according to the best of our knowledge. In fact, intercomparisons of electron densities measured in the Martian ionosphere by different instruments appear to be rather rare. This may be due to the fact that the measurements seldom take place at comparable times and locations, resulting in natural discrepancies because of different data coverage both in space and time, which are difficult to account for. Vogt et al. (2016) compared electron densities determined from the MARSIS radar sounding with Mariner 9, Viking, and Mars Global Surveyor radio occultation experiments. They showed that the MARSIS data agree well with the radio occultation measurements close to the peak altitude. However, at higher altitudes, MARSIS-derived electron densities are consistently larger than the radio occultation densities. This is probably due to a bias in the MARSIS electron density profiles related to a detection threshold of the radar sounding and associated ambiguities in the ionospheric trace inversion (Němec, Morgan, Gurnett, 2016).

The presented study uses MARSIS radar sounding and LPW electron density data for two main purposes:

1. MAVEN has lower perigee than Mars Express, and it thus allows us to conveniently cover the altitude region where the electron densities cannot be locally evaluated by MARSIS nor measured — due to the lower detection threshold — by the MARSIS radar sounding. The relevant LPW measurements are statistically evaluated to derive an empirical electron density profile shape in this MARSIS return signal gap region and to increase the overall quality of the MARSIS electron density profiles.
2. We perform the first direct comparison of MARSIS and LPW electron density measurements in order to demonstrate whether the electron density profiles derived from the two instruments via different physical principles are in good agreement or not. Here we use the time intervals that coincident observations are available when the two instruments are located within a 5° SZA interval within 1 h.

The MARSIS and LPW electron density measurements used in the present analysis are briefly described in section 2. The results obtained concerning the transition region and the improvement of the MARSIS ionospheric trace inversion are presented in section 3. Coincident observations of approximately the same ionospheric region within a 1 h time interval both by Mars Express and MAVEN spacecraft are described in section 4. The obtained results are discussed in section 5. Finally, the main results are briefly summarized in section 6.

2. Data Set

The Mars Express spacecraft has an eccentric orbit with an inclination of 86° and an orbital period of about 7 h. The spacecraft orbit evolved slightly during the mission duration, with the periapsis altitude typically about 300 km and the apoapsis altitude of more than 10,000 km. The MARSIS instrument on board was designed for ionospheric and subsurface radar sounding (Gurnett et al., 2005; Jordan et al., 2009; Picardi et al., 2004). In the ionospheric sounding mode, the time delay Δt until the sounding signal is reflected from the ionosphere and detected by the instrument receiver is measured as a function of the sounding signal frequency f. The $\Delta t(f)$ dependence can be then "inverted" to obtain an electron density profile from the spacecraft altitude down to the altitude of the peak electron density in the ionosphere (Morgan et al., 2008, 2013). However, due to the low power radiated by the instrument antenna at low frequencies, the ionospheric reflections at low sounding frequencies are generally not detected. This effectively corresponds to a return signal gap between the locally evaluated electron density (Duru et al., 2008) and the lowest electron density detectable by the radar sounding (about 10^4 cm^{-3}; see Němec et al., 2010). As a consequence, the inversion process is

not unambiguous, and a unique solution is found by assuming a predefined electron density profile shape in the return signal gap region (Němec, Morgan, Gurnett, 2016). The electron densities are generally assumed to monotonically increase with decreasing altitude down to the altitude of the peak; that is, any density voids in the altitude profile/transient layers (Kim et al., 2012; Kopf et al., 2008; Withers, Fillingim, et al., 2012) cannot be evaluated.

Following Morgan et al. (2008), only the MARSIS ionospheric traces that meet the predefined quality criteria were included in this analysis. The following conditions have been imposed. (1) The spacecraft altitude at the time of the measurement must be lower than 500 km in order to minimize the return signal gap. (2) The maximum gap in the detected ionospheric trace must be less than 0.4 MHz, in order to avoid large gaps in the ionospheric trace. (3) The maximum allowed jump in delay time is 0.2 ms, in order to avoid the ionospheric cusps indicative of transient layers (Kopf et al., 2008). (4) The time delay of the ionospheric trace at the highest sounding frequency point must be larger than the time delay at the frequency point just before, in order to ensure that the trace ends with a discernible cusp. (5) Maximum detected frequency of the ionospheric trace must not be within 2.25 MHz and 2.30 MHz, in order to avoid falling in the receiver gap known to exist in this frequency range. (6) The minimum frequency of the ionospheric trace must be lower than 1.27 MHz (corresponding to the electron density of 2×10^4 cm^{-3}), in order to minimize the return signal gap and ensure a reasonable length of the ionospheric traces. (7) The resulting electron density profiles must be monotonic, which is occasionally not the case for ionospheric traces with a sudden decrease in the time delay. (8) The SZA of the spacecraft at the time of the measurement must be lower than 80°, in order to avoid low electron densities and possible further complications close to the terminator (Duru et al., 2010). Altogether, 27,629 electron density profiles that fulfill the aforementioned conditions were measured by the MARSIS instrument from July 2005 until the end of 2015, digitized, and included in the analysis. We note that this corresponds to only about 10% of the total number of digitized ionospheric traces. Unfortunately, the remaining measurements cannot be used to derive reliable electron density profiles.

The MAVEN spacecraft has a periapsis altitude of about 150 km, and the apoapsis altitude of some 6,200 km (Jakosky et al., 2015). The orbital inclination is about 70°, and the orbital period is about 4.5 h. The LPW instrument consists of two independent probes that measure the current-voltage (*I-V*) dependence, one after the other in time. The electron densities and temperatures used in this study are derived from fitting the *I-V* curves, resulting in the most likely values ("main values") and their lower and upper estimates. As the two probes have minor differences in probe properties, the main values obtained from the two probes are slightly different but well within the upper and lower estimates of the two derived quantities. In order not to be distracted by this, only data from boom 1 are used in the present study. The usage of boom 1 is recommended by the LPW instrument team for two reasons: (i) it is capable to measure slightly lower temperatures (down to $\approx$ 525K as compared to $\approx$ 700K for boom 2; Ergun et al., 2015), and (ii) science quality electron densities and temperatures from boom 2 are only sporadically available after mid-2015 due to operational difficulties. The LPW instrument can also derive the local electron density based on wave sounding of the local plasma line. However, the upper frequency range of the measurements limits the measurable densities to below about 2.3×10^4cm^{-3} (Fowler et al., 2017). This upper density limit is too low to allow for an intended comparison with the MARSIS data. Further, the wave-derived electron densities are not regularly available after mid-December 2015 due to a change in the instrument operation mode. The electron densities derived from the wave sounding were thus not used in this study. A more detailed description of the LPW instrument was given by Andersson et al. (2015).

MARSIS electron density profile parts based on the radar sounding have typically altitudes lower than about 250 km. At higher altitudes, electron densities are below the lower detection threshold of the MARSIS radar sounding. Further, electron densities at altitudes higher than about 325 km generally follow a simple exponential decrease with the altitude (e.g., Duru et al., 2008, 2011), which has been statistically well mapped using the MARSIS locally evaluated electron densities (Andrews et al., 2015; Němec et al., 2011). In the present study, LPW electron density measurements are important for the two main reasons: (i) Due to the lower perigee of MAVEN as compared to Mars Express, they allow us to fill the altitudinal gap between the MARSIS radar sounding and MARSIS locally evaluated electron densities, and (ii) at lower altitudes, one can compare LPW in situ measurements with electron density profiles obtained by the MARSIS radar sounding. Only the LPW electron densities measured at altitudes lower than 325 km are thus used in the present study. Altogether, 1,012,433 data points measured between October 2014 and January 2017 were included in the analysis.

3. Empirical Dependence in the Transition Region

Electron densities corresponding to plasma frequencies between the local plasma frequency and the lowest frequency detectable by the ionospheric sounding are not measured by the MARSIS instrument. However, they affect the interpretation of sounding signals at higher frequencies, and their knowledge is thus needed to properly calculate electron density profiles from MARSIS ionospheric traces. As discussed in detail by Němec, Morgan, Gurnett (2016), this limitation of the MARSIS instrument can be partly overcome by assuming a reasonable electron density profile shape in the return signal gap region. Following former statistical results on electron density profile shapes (Němec et al., 2011), they suggested to use an empirical shape composed of a smooth transition between two exponential dependencies with different scale heights, with the scale height H_2 at higher altitudes being larger than the scale height H_1 at lower altitudes (Gurnett et al., 2005; Morgan et al., 2008):

$$\ln n_e = C + \frac{\theta_1 + \theta_2}{2}(z - z_0) + \frac{\theta_2 - \theta_1}{2}\sqrt{(z - z_0)^2 + \frac{\delta^2}{4}} \quad (1)$$

where $\theta_1 = 1/H_1$, $\theta_2 = 1/H_2$, z_0 is a transition altitude corresponding to the altitude where the two asymptotic dependencies intersect, δ is a quantity proportional to the radius of curvature, and C is a constant. The value of θ_2 can be adopted from statistical models of electron density scale height at high altitudes (Andrews et al., 2015; Němec et al., 2011). For given values of z_0 and δ, the values of C and θ_1 are then unambiguously given by the conditions that (i) the electron density at the spacecraft altitude must be equal to the one actually measured, and (ii) the measured time delay at the lowest frequency available from the ionospheric sounding must be equal to the time delay calculated using the empirical electron density profile. However, the values of z_0 and δ remain somewhat arbitrary, and it is difficult to obtain them exclusively using the MARSIS measurements. Němec, Morgan, and Gurnett (2016) attempted to estimate them using a correlation analysis, arguing that the calculated peak ionospheric altitude should be independent of the Mars Express altitude at the time of the measurement. They noted that a range of possible combinations leads to comparable results, and they eventually adopted the values of $z_0 = 275$km and $\delta = 55$ km.

In the present analysis, we use the MAVEN LPW data to get an estimate of these crucial parameters directly from in situ measurements. As the MAVEN LPW data provide a good coverage of the density (altitude) region not accessible by MARSIS, the values of z_0 and δ can be obtained from a fitting of the observed electron density dependencies. This is demonstrated in Figures 1 and 2.

As preliminary results from the MAVEN LPW instruments seem to suggest that the ionospheric electron densities are significantly different on the dawnside than on the duskside (Benna et al., 2015), we plot the dependencies for the morning and afternoon regions separately. Specifically, Figure 1 shows the results obtained for the Mars-centered solar orbital (MSO) local time interval 6–12 h ("morning"), while Figure 2 shows the results obtained for the MSO local time interval 12–18 h ("afternoon"). The format of both figures is the same. Each of Figures 2a–2f was obtained for a different range of SZAs. These are marked at the top left of each of the panels. Probability of LPW measuring an electron density in a given density bin at a given altitude is color coded according to the scale on the right-hand side. The thick black curves show the median dependencies. Note that the dependencies are plotted only for median electron densities lower than 20,000 cm^{-3}. This threshold was chosen, as it is typically well above the lowest electron densities detectable by the MARSIS radar sounding (Němec et al., 2010); that is, there is no need to derive an empirical electron density profile shape at larger electron densities. Moreover, the electron density profile shape at larger electron densities changes to approximately follow the Chapman-like profile close to the ionospheric peak, and its approximation by the empirical curve described by equation (1) is thus no longer valid.

Our aim is to find the values of parameters z_0 and δ that would result in empirical profile shapes described by equation (1) to be close to the median dependencies derived using the LPW electron density measurements. Although one might consider these values to depend on SZA, local time, and possible other parameters, it turns out that very good agreement between the median dependencies and empirical profile shapes can be achieved already using constant values of z_0 and δ. We have determined these constants in order to result in the best overall agreement, that is, in order to minimize the sum of squared differences from the black median curves in Figures 1 and 2. This fitting procedure resulted in $z_0 = 185$km and $\delta = 107$km. The obtained

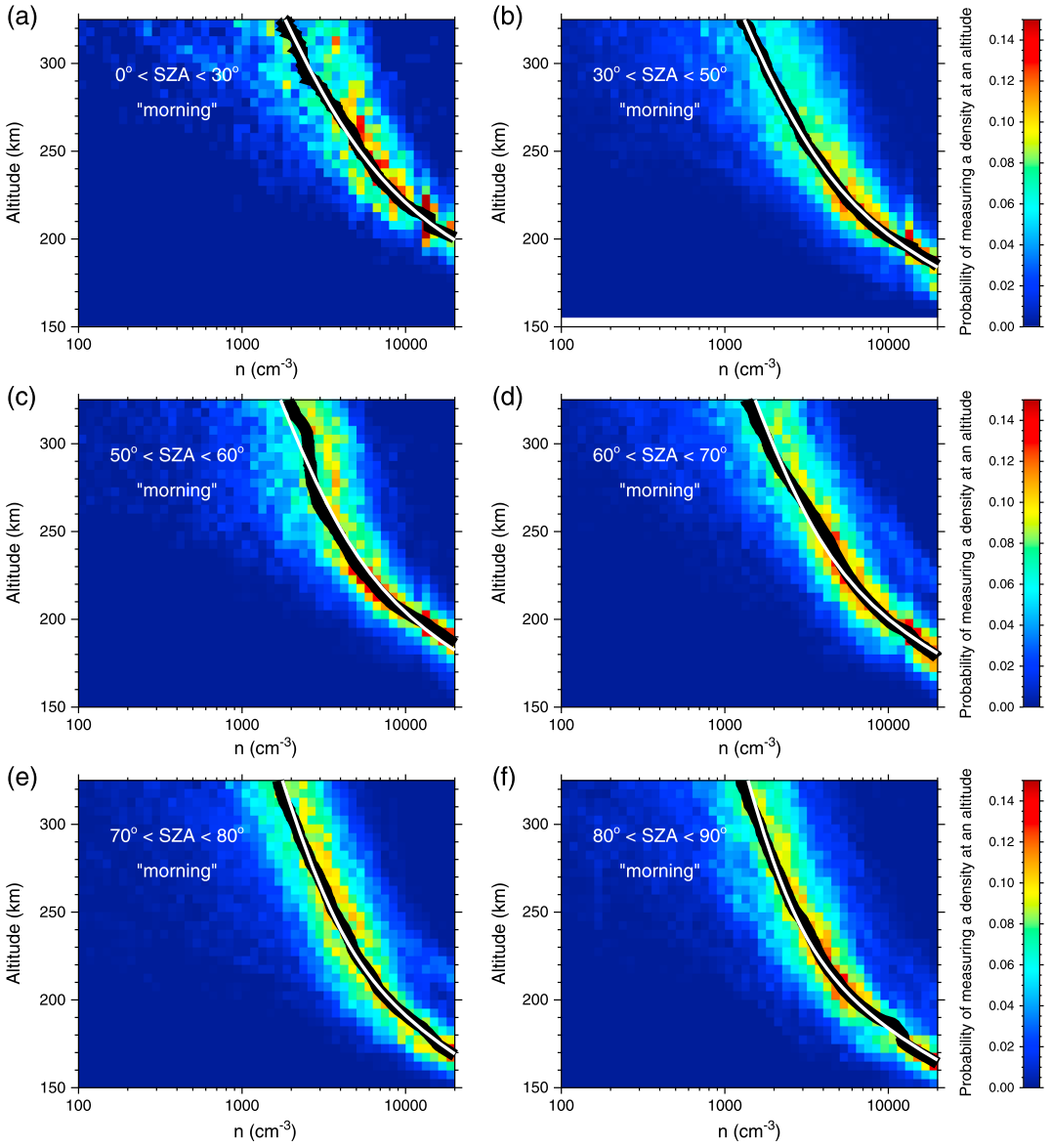

Figure 1. (a)–(f) Probability of LPW measuring an electron density in a given density bin at a given altitude is color coded according to the color scale on the right-hand side. Only measurements at Mars-centered solar orbital (MSO) local times 6–12 h were used. The thick black curves show the median altitudinal dependencies of the electron density. The white curves show the empirical fits using the hyperbola transition between two exponential dependencies (see text). Individual panels were obtained for different SZA intervals. These are stated at the top left of each of the panels.

empirical dependencies are plotted by the white curves in Figures 1 and 2. The value of H_2 was determined using the empirical relation given by Andrews et al. (2015) as

$$\log_{10}(H_2) = 2.61 - 0.572 \tanh\left(-\frac{\mathrm{SZA} - 107.0}{34.3}\right) \quad (2)$$

where H_2 is in kilometers and SZA is in degrees. The values of C and $\theta_1 = 1/H_1$ were determined for each SZA and morning/afternoon interval in order to result in the best fit. It can be seen that the used constant values of z_0 and δ result in empirical dependencies well fitting the observations over all the analyzed range of SZAs and both during the morning and afternoon periods. Although the median dependencies observed during the morning and afternoon are significantly different, with the morning density profiles being generally more steep, the constant values of z_0 and δ work both for morning and afternoon. This is allowed by a different fitted asymptotic slope at low altitudes, $H_1 = 1/\theta_1$, which is steeper during the morning than during the afternoon.

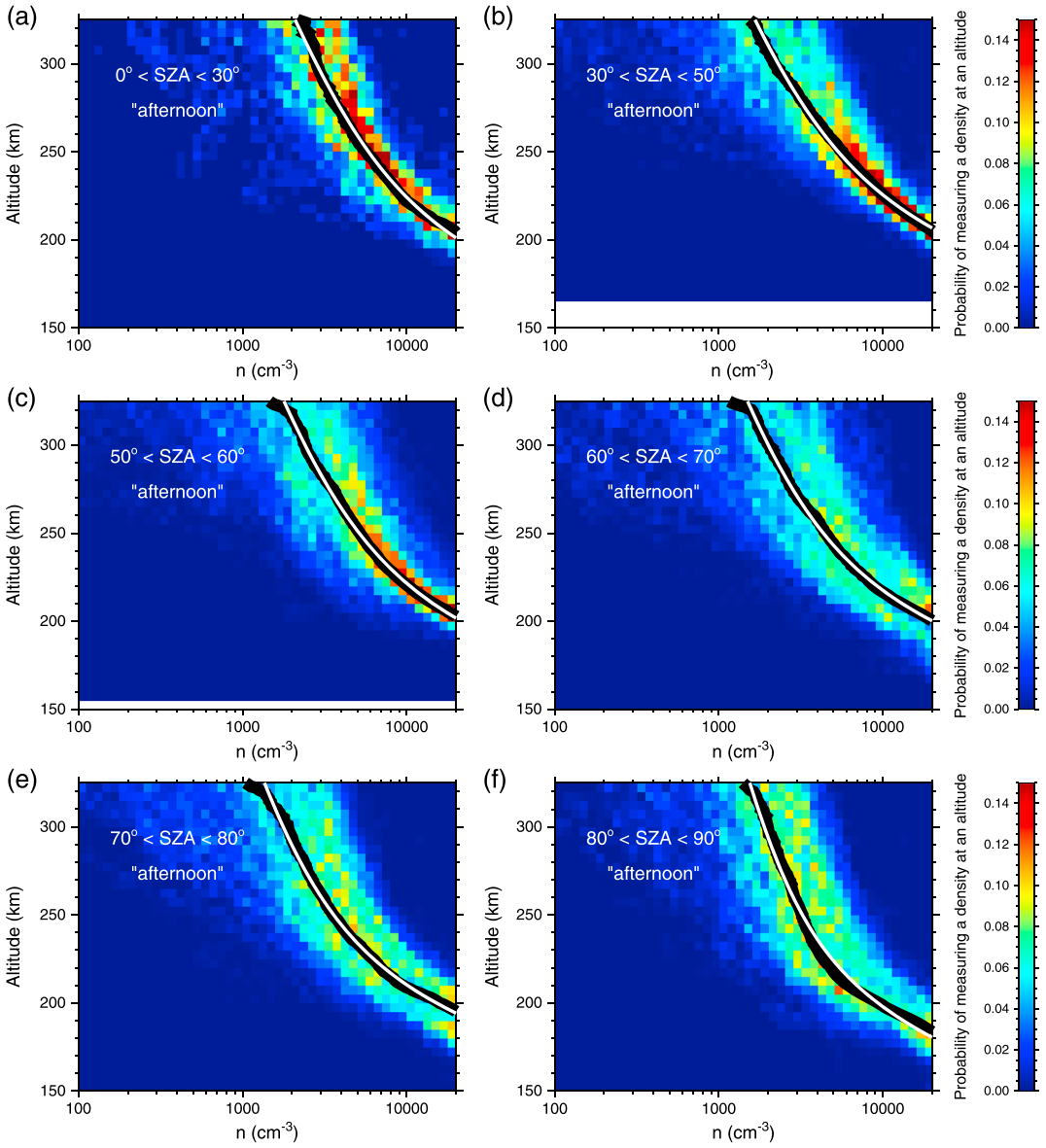

Figure 2. The same as Figure 1 but for the MSO local times 12–18 h.

We note that when using the empirical electron density profile shape to invert MARSIS ionospheric traces, the values of H_1 are determined directly from the measured data.

Introducing the newly derived parameters of the empirical electron density profile shape in the transition region not covered by the MARSIS radar sounding in the trace inversion routine suggested by Němec, Morgan, Gurnett (2016) allows us to improve the overall quality of MARSIS electron density profiles. An example of a comparison between the electron density profiles obtained using the old and new parameters is shown in Figure 3. Electron density profiles based on the MARSIS measurements performed at two representative time intervals are shown. Figure 3a was obtained using the data measured on 23 September 2005 at 18:02:56 UT and SZA of 33.3°. The electron density profile obtained using the parameters of the empirical profile shape derived in the present paper is shown by the red curve. The electron density profile obtained using the original empirical profile shape parameters derived by Němec, Morgan, Gurnett (2016) is shown by the blue curve. Finally, the black curve shows the electron density profile obtained using a simple exponential interpolation. It can be seen that the difference between the individual curves is not very large. This is because the analyzed time interval corresponds to a situation of rather large electron densities, when the altitude of the first data point available from the ionospheric sounding is high as compared to the transition altitude. In such a

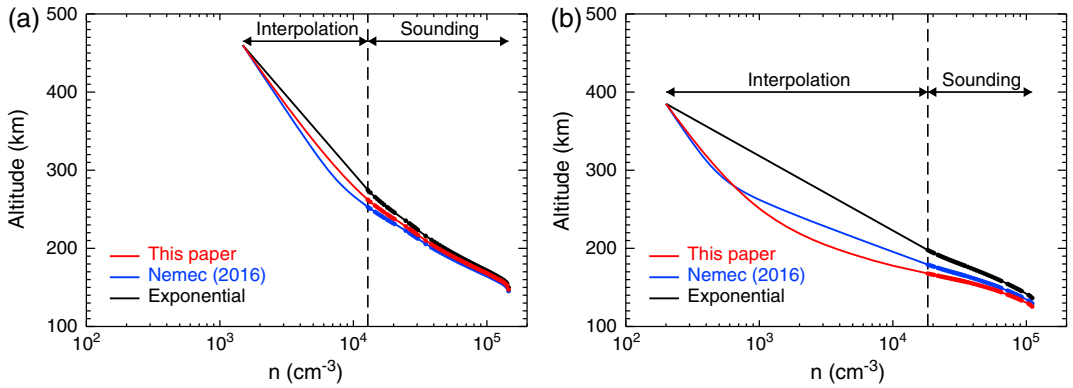

Figure 3. (a) Comparison of MARSIS electron density profiles obtained using the new empirical profile shape parameters (red curve), original empirical profile shape parameters derived by Němec, Morgan, Gurnett (2016) (blue curve), and a simple exponential interpolation (black curve). The measurement was performed on 23 September 2005 at 18:02:56 UT and SZA of 33.3°. The vertical dashed line marks the density threshold of the radar sounding. The parts of electron density profiles at lower electron densities are based on the assumed empirical profile shapes, while the parts of electron density profiles at larger electron densities were obtained from the radar sounding. The electron densities corresponding to the discrete frequencies of the MARSIS sounding signal are marked by the small solid points. (b) The same as Figure 3a but for the measurement performed on 17 February 2008 at 21:52:40 UT and SZA of 48.3°.

case, only the high-altitude exponential part of the empirical profile is used; that is, the method effectively converges to a simple exponential interpolation.

Figure 3b obtained using the data measured on 17 February 2008 at 21:52:40 UT and SZA of 48.3° shows a rather different picture. In this case, the overall electron densities are lower, and the first data point available from the ionospheric sounding is at a rather low altitude, increasing thus the importance of a reasonable empirical profile shape in the return signal gap region. It can be seen that the red curve represents arguably the most realistic profile shape. Specifically, the transition altitude $z_0 = 275$km used by Němec, Morgan, Gurnett (2016) appears to be too high. This is the case both when comparing with the radio occultation results (Vogt et al., 2016) and with the recently available MARSIS measurements, as well as with simple theoretical estimates based on the evaluation of diffusive and photochemical timescales (Withers, 2009). All these independent estimates indicate that the transition altitude should be at about 200 km. We note that although the shapes of electron density profiles at large electron densities (low altitudes) are not too affected by an empirical profile shape assumed in the return signal gap region, all the high-density parts of the profiles may effectively shift in the altitude. The newly derived parameters of the empirical electron density profile shape result in the peak altitude difference generally within about 4 km (median −0.4km, mean −0.6km) as compared to the original values derived by Němec, Morgan, Gurnett (2016). Considering that the uncertainty in the MARSIS ionospheric trace delay times corresponds to about 13.7 km (Morgan et al., 2013), this difference in the determined peak altitudes is very small, and possibly significant only when many traces are analyzed in a statistical manner. However, the difference between the profiles at higher altitudes is progressively larger (see Figure 3b).

4. Coincident Observations

Coincident MARSIS and LPW electron density measurements can be used to understand how the data sets overlap and to provide different views of the same ionosphere. In order to do so, we would ideally need to select the time intervals when the spacecraft were close to each other both in time and space. However, as this is very difficult to achieve, we slightly relax this condition. Specifically, we require the MARSIS and LPW measurements to be taken within 1 h and with the SZA difference less than 5°. No condition on the relative geographic location is set; that is, the measurements can be performed rather far from each other, as long as they are performed at about the same SZA. Altogether, four relevant time intervals were identified and analyzed in detail. These are shown in Figures 4–7, respectively. The format is the same for all the figures. The color curves in Figures 4a, 5a, 6a, and 7a show electron density profiles obtained from the MARSIS radar sounding. The dotted parts of the curves mark the parts of the profiles that are below the lower detection limit of the ionospheric sounding; that is, they correspond to the aforementioned empirical profile shapes. The solid

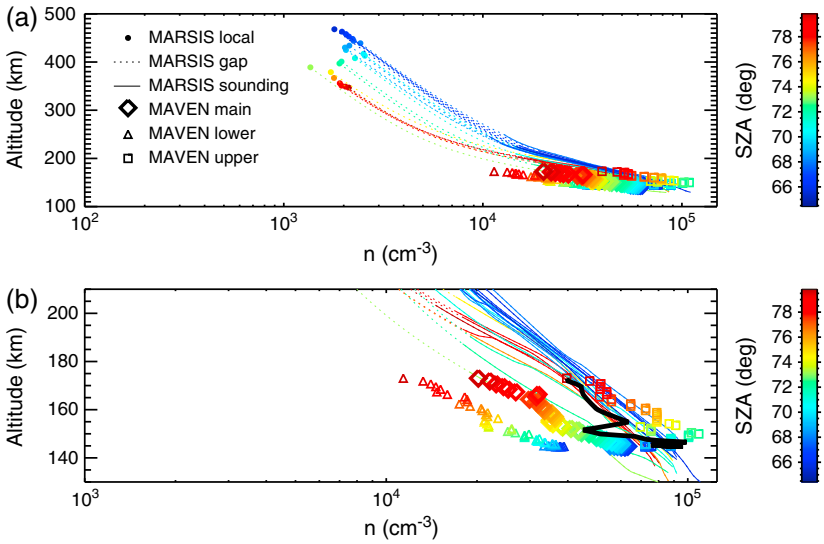

Figure 4. (a) The color curves show electron density profiles obtained by the MARSIS instrument on 2 October 2015 between 00:36:11 UT and 00:40:20 UT. The dotted parts of curves mark the parts of the electron density profiles not accessible by the ionospheric sounding, that is, based on the empirical electron density profile shape. The solid parts of the curves mark the parts of the electron density profiles determined from the ionospheric sounding. The solid points at the top of each of the profiles correspond to MARSIS local electron density measurements. SZAs of individual electron density profiles are color coded according to the color scale on the right-hand side. The colored diamonds, triangles, and squares correspond to LPW electron density measurements and their lower and upper uncertainty estimates, respectively. These were obtained on 2 October 2015 between 00:18:11 UT and 00:21:39 UT. The appropriate SZAs are again color coded according to the color scale on the right-hand side. (b) A zoom of the low-altitude part of Figure 4a. The used format is the same. Additionally, the black curve shows a prediction of the LPW electron density measurements based on the MARSIS data.

points at the top of each of the profiles correspond to MARSIS local electron density measurements. The LPW electron density measurements and their lower and upper estimates are marked by the diamond, triangle, and square symbols, respectively. SZAs of individual measurements are color coded according to the scale on the right-hand side. Figures 4b, 5b, 6b, and 7b are zooms of low-altitude parts of Figures 4a, 5a, 6a, and 7a. Additionally, the black curves in Figures 4b, 5b, 6b, and 7b show predictions of LPW electron density measurements based on the evaluation of the MARSIS data. These were obtained from the MARSIS-derived electron densities at the MAVEN altitudes. Given that the MARSIS measurements were not performed at exactly the same SZAs as the MAVEN measurements, an interpolation of the MARSIS measurements performed at SZAs just below and just above the SZAs of the MAVEN spacecraft was used to obtain the MARSIS-based estimates of electron densities at MAVEN locations. Note that no LPW measurements are shown at altitudes above about 200 km, as—for the four analyzed coincident events—these were measured at SZAs larger than 80°, and they thus do not meet the aforementioned selection criteria.

The data depicted in Figure 4 were obtained on 2 October 2015. The relevant MARSIS data were obtained within a 4 min interval between 00:36:11 UT and 00:40:20 UT. The spacecraft latitude at this time interval was between −59.3° and −43.6°, and the spacecraft east longitude was between 116.9° and 118.1°. The corresponding LPW electron density measurements were performed on the same day between 00:18:11 UT and 00:21:39 UT. The latitude of the MAVEN spacecraft at this time interval was between −58.2° and −45.6°, and the east longitude of the MAVEN spacecraft was between 115.3° and 124.9°. The two spacecraft thus flew over the very same region, with a time delay between MAVEN and Mars Express of about 20 min. The LPW electron density measurements agree reasonably well with the MARSIS electron density profiles, but they tend to be somewhat lower, with the MARSIS electron densities in between the LPW electron densities and their upper estimates.

Figures 5 and 6 show roughly the same picture obtained for two other events. The first of them occurred on 2 October 2015, with the MARSIS data measured between 14:35:15 UT and 14:39:17 UT, and the LPW data measured between 13:57:10 UT and 14:00:34 UT. At the given time interval, the Mars Express spacecraft was located at the latitude between about −59.6° and −44.4°. The east longitude of the spacecraft was between

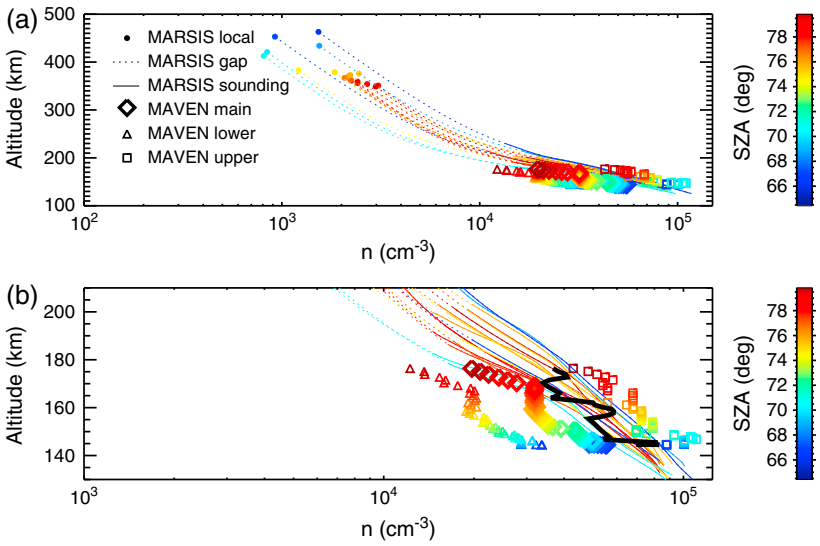

Figure 5. The same as Figure 4 but for MARSIS measurements on 2 October 2015 between 14:35:15 UT and 14:39:16 UT and LPW measurements on 2 October 2015 between 13:57:10 UT and 14:00:34 UT.

about 272.3° and 273.6°. The MAVEN spacecraft at the time of the LPW measurements of interest was located at the latitude between about −58.6° and −46.2° and east longitude between about 275.7° and 285.4°. This means that, again, the two spacecraft flew above nearly the same region, with the MAVEN spacecraft being about 38 min ahead. The second event occurred on 4 October 2015, with the MARSIS data measured between 01:33:52 UT and 01:37:30 UT, and the LPW data measured between 02:19:53 UT and 02:22:57 UT. At the time of the measurements, the Mars Express spacecraft was located at the latitude between about −56.1° and −42.5° and east longitude between about 121.5° and 122.4°. At the time of the LPW measurements of interest, the MAVEN spacecraft was located at the latitude between about −56.0° and −44.7° and east longitude between about 102.0° and 109.8°. Although the two spacecraft were thus separated by some 15° in longitude, they were still reasonably close to each other, with the MAVEN spacecraft being by about 45 min ahead of Mars Express.

The event depicted in Figure 7 appears to result in the best overall agreement between the MARSIS and LPW electron density measurements. It occurred on 6 October 2015, with the MARSIS data measured between 09:29:33 UT and 09:33:27 UT, and the LPW data measured between 08:55:55 UT and 08:59:15 UT. At the time

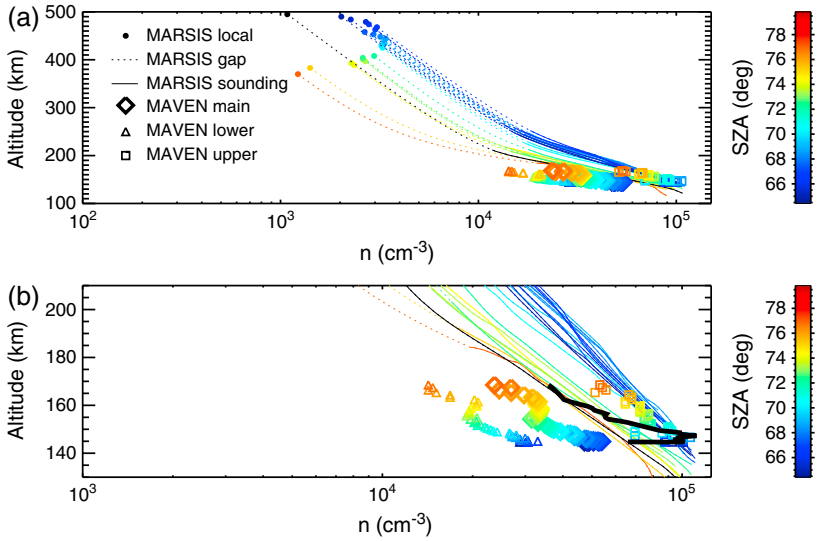

Figure 6. The same as Figure 4 but for MARSIS measurements on 4 October 2015 between 01:33:52 UT and 01:37:30 UT and LPW measurements on 4 October 2015 between 02:19:53 UT and 02:22:57 UT.

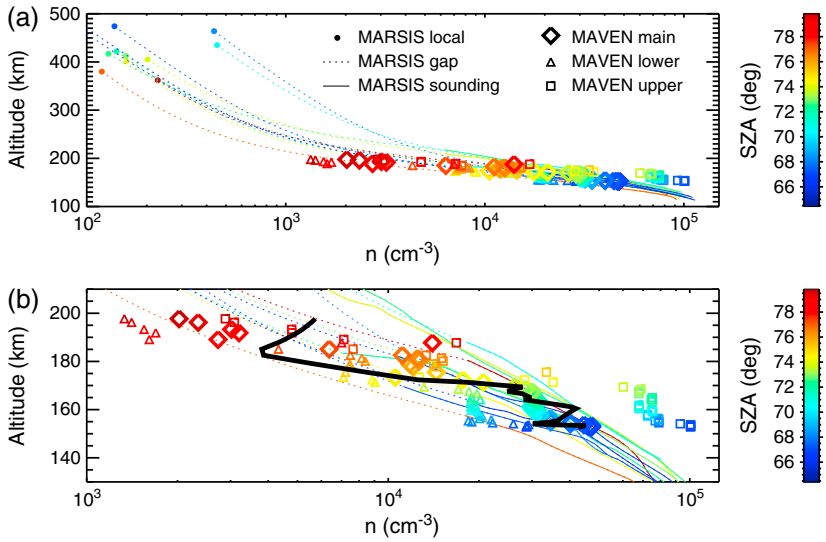

Figure 7. The same as Figure 4 but for MARSIS measurements on 6 October 2015 between 09:29:33 UT and 09:33:27 UT and LPW measurements on 6 October 2015 between 08:55:55 UT and 08:59:15 UT.

of the measurements, the MARSIS spacecraft was located at the latitude between about −58.9° and −44.3° and east longitude between about 23.1° and 24.3°. At the time of the LPW measurements of interest, the MAVEN spacecraft was located at the latitude between about −58.5° and −46.5° and east longitude between about 23.3° and 32.7°. The two spacecraft thus flew above approximately the same region, with the MAVEN spacecraft being some 35 min ahead of Mars Express.

The overall agreement between the MARSIS and LPW electron density measurements is analyzed in Figures 8 and 9. Figure 8 shows a direct comparison of LPW and MARSIS electron density measurements (interpolated to the MAVEN SZAs, i.e., the black curves from Figures 4–7). The lower and upper uncertainties of LPW electron density measurements are shown by the vertical error bars. The SZAs of the MAVEN spacecraft at the times of the measurements are color coded according to the scale on the right-hand side. The diamond, triangle, square, and cross symbols correspond to the first, second, third, and fourth event, respectively. The diagonal dashed line shows a 1:1 dependence. It can be seen that the MARSIS and LPW electron densities agree remarkably well. The large cluster of data points at larger electron densities is on average slightly below the dashed line, corresponding to the MAVEN electron densities systematically somewhat below the MARSIS electron densities, consistent with the aforementioned results. The data points at low electron densities ($< 10^4 cm^{-3}$) are below the detection threshold of the MARSIS ionospheric sounding; that is, the appropriate MARSIS electron densities were obtained using the empirical electron density profile shape smoothly transiting between the locally measured electron density at the Mars Express spacecraft location and the first data point from the MARSIS ionospheric sounding.

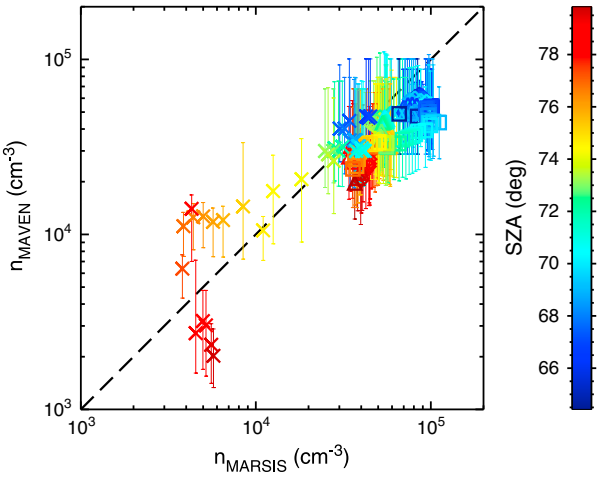

Figure 8. Electron densities measured by the LPW instrument as a function of corresponding electron densities evaluated for the appropriate altitudes and SZAs based on the MARSIS electron density profiles. The vertical error bars show the uncertainties of the LPW electron density measurements. The data points corresponding to the events from Figures 4–7 are shown by the diamonds, triangles, squares, and crosses, respectively. The color of individual symbols corresponds to the SZA of the measurements, using the color scale on the right-hand side.

A histogram of the ratios between the LPW and MARSIS electron densities is shown in Figure 9 by the black line. The blue and red lines show, respectively, the histograms obtained using the LPW lower and upper electron density estimates. The vertical dashed lines of respective colors correspond to appropriate median values. The LPW electron densities are on average somewhat lower than those determined using the MARSIS data (median electron density ratio of about 0.73). However, considering the lower and upper uncertainties of the LPW measurements, the two data sets are well consistent (median ratio value obtained using the LPW lower electron density estimates is about 0.43, median ratio value obtained using the LPW upper electron density estimates is about 1.44).

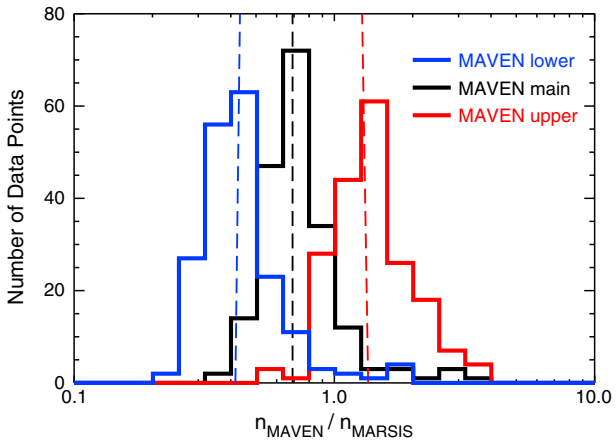

Figure 9. Histogram of the ratios between LPW electron densities and corresponding electron densities evaluated for the appropriate altitudes and SZAs based on the MARSIS electron density profiles. The blue, black, and red histograms were obtained using LPW lower electron density estimates, main electron density estimates, and upper electron density estimates, respectively. The color vertical dashed lines mark the median values of the respective distributions.

5. Discussion

The low power radiated by the MARSIS radar sounder at low sounding frequencies and the associated return signal gap represent a considerable complication when performing the trace inversion, that is, when recalculating the measured ionospheric traces into electron density profiles. Specifically, electron density profiles in the density range between the local electron density and the lowest electron density detectable by the ionospheric sounding cannot be deduced using the MARSIS data. The inversion of MARSIS ionospheric traces is thus ambiguous. Moreover, considering the dispersion of the sounding signal, the ambiguity not only concerns the low-density parts of electron density profiles but also effectively affects the entire profile. Although the profile shape at higher electron densities (low altitudes) is not very sensitive to the exact choice of the electron profile shape in the return signal gap region, the profile as a whole can effectively move to higher/lower altitudes by as much as 5 km. At higher altitudes (lower electron densities) the difference is generally larger (see Figure 3). As the primary purpose of the MARSIS radar sounding is to obtain electron density profiles, and the large amount of MARSIS radar sounding data collected to date is used to construct/validate models and statistics of the Martian ionospheric electron densities (Sánchez-Cano et al., 2013; Morgan et al., 2008; Němec et al., 2011), it is important to tune the inversion procedure to obtain as reliable electron density profiles as possible. This is particularly striking when analyzing the MARSIS electron density profiles in a statistical manner, as unrealistic profile shapes in the return signal gap region may result in a systematic bias in derived altitudes (Němec, Morgan, Gurnett, 2016). The formerly considered unrealistic profile shapes are also a reason for the discrepancies between MARSIS and radio occultation electron density data sets reported by Vogt et al. (2016) at higher altitudes.

It is thus of the utmost importance to estimate the profile shape in the return signal gap region as well as possible. The profile shape suggested by Němec, Morgan, and Gurnett (2016) and the related trace inversion routine respect long-term statistical dependencies derived for the high-altitude diffusion region, and, moreover, it can be easily used for the inversion of MARSIS ionospheric traces. The two parameters describing the profile shape in this region, namely the transition altitude z_0 and the radius of curvature δ, cannot be directly determined using the MARSIS data. However, the availability of the MAVEN LPW electron density data allowed for their direct evaluation. We determined the optimal values of these parameters in such a way that the resulting empirical electron density profiles closely follow the long-term LPW dependencies. The used approach demonstrates clearly the advantage of using the LPW electron density data set along with the MARSIS measurements. We note that the revised trace inversion routine based on the LPW-determined parameters is on average optimal, in the sense that the obtained results follow the expected long-term distributions. Nevertheless, in individual cases, the actual profile shapes in the return signal gap region may differ significantly from the long-term average, and the used trace inversion routine would thus result in not entirely correct electron density profiles. This is a principal limitation stemming from the MARSIS data, and it cannot be overcome.

It is important to perform a direct comparison of LPW and MARSIS electron densities, in order to verify their correctness and identify any possible biases. Given that the instruments orbit on two different spacecraft, it is principally impossible for them to occur at exactly the same location. However, considering that SZA and the incoming solar radiation flux are the most important controlling factors of the Martian daytime ionosphere (e.g., Němec et al., 2011; Withers, 2009), we can focus on the analysis of the time intervals when the spacecraft are located at about the same SZAs. The approximately same times of the measurements then ensure that the solar radiation flux and the Sun-Mars distance are basically the same. However, the spacecraft may be located at different geographic locations, with different local conditions and with different configuration and magnitude of the crustal magnetic fields.

Nevertheless, the LPW electron densities are in agreement with the MARSIS electron densities in all analyzed coincident events. They are on average somewhat lower than the MARSIS electron densities, but the difference is well within the uncertainty range. Apart from the Langmuir probe measurements, there are also other measurements on board MAVEN that can be used to derive plasma densities, such as the wave measurements,

neutral gas and ion mass spectrometer, and the low-energy ion detector. All these suggest that at high densities the Langmuir probe measurements are on the high-density ends. We note in this regard that it is difficult to evaluate the uncertainty of the MARSIS electron density measurements. Due to the inversion process and the necessity to derive the corrected altitude range, the uncertainty of the resulting electron density profiles is primarily altitudinal. Should the possible overestimation of MARSIS electron densities as compared to the LPW measurements be a MARSIS issue, it would thus likely correspond to MARSIS electron density profiles being on average slightly "too high," that is, with the assumed electron density profile shape in the return signal gap region not steep enough. Although the assumed profile shape corresponds to the long-term average, it is possible that in the few analyzed events the situation was rather different.

The observed differences between LPW in situ electron density measurements and MARSIS electron density profiles vary significantly from event to event and as a function of the altitude. This remains the case even when the effect of the LPW measurements being made at different SZAs is taken into account, as presented in Figures 4–7 when comparing the black curves with the diamonds. However, the discrepancies observed in Figures 4–7 are typically within the uncertainty in the LPW measurements. Considering that LPW and MARSIS are two different instruments with completely different physical principles placed on board two different spacecraft, the overall agreement of the measured electron densities is surprisingly good.

6. Conclusions

We have presented the first direct comparison of electron density measurements in the Martian ionosphere performed by the MARSIS instrument on board the Mars Express spacecraft and by the LPW instrument on board the MAVEN spacecraft, demonstrating a reasonable agreement between the two data sets. The in situ measured LPW electron densities were also used to improve the empirical profile shape in the altitudinal region not covered by the MARSIS data, allowing to obtain more reliable MARSIS electron density profiles.

Due to the low power radiated by the MARSIS radar sounder at low frequencies, it is generally not possible to evaluate the low-density parts of electron density profiles from the measured data. Instead, one needs to assume a reasonable electron density profile shape in the return signal gap region between the local electron density and the lowest electron density detectable by the radar sounding. We demonstrated that the MAVEN LPW electron density measurements can be efficiently used to determine an optimal shape of this electron density profile. Although a significant morning-afternoon asymmetry was identified in the MAVEN LPW data set, the return signal gap region can be described by a single formula. We derived the values of its parameters, and we used the revised trace inversion procedure to improve the accuracy of the MARSIS electron density profiles.

We further focused on a direct comparison between the MARSIS and LPW electron densities during coincident events. Four events when the Mars Express and MAVEN spacecraft were within a 5° SZA interval during a 1 h time interval were identified and analyzed. We showed that there is a good agreement between the electron density measurements performed by the two instruments. The MAVEN electron densities are typically slightly lower than those obtained by MARSIS but within the uncertainties.

The obtained results allow us to improve the precision of the electron density profiles obtained by the MARSIS instrument on board Mars Express. The calculated electron densities are in agreement with the electron densities measured locally by the LPW instrument on board the MAVEN spacecraft. Further, preferentially large-scale, intercomparison between various electron density data sets is surely desirable, as it would allow both to evaluate possible biases in individual instrument data and to better understand the ionospheric variability. Given the ionospheric variability as a function of—among others —the solar cycle, solar longitude, SZA, and location, and uncertainties in the absolute density of the in situ measurements and the altitude determined from the remote sounding, it may be, however, difficult to achieve.

Acknowledgments
MARSIS data are available via the ESA Planetary Science Archive (http://www.rssd.esa.int/PSA). MAVEN LPW data are available via the Planetary Data System (https://pds-ppi.igpp.ucla.edu/). F. N. acknowledges the support of the MSMT INTER-ACTION grant LTAUSA17070.

References

Andersson, L., Ergun, R. E., Delory, G. T., Eriksson, A., Westfall, J., Reed, H., … Meyers, D. (2015). The Langmuir Probe and Waves (LPW) instrument for MAVEN. *Space Science Reviews*, *195*, 173–198. https://doi.org/10.1007/s11214-015-0194-3

Andrews, D. J., Opgenoorth, H. J., Edberg, N. J. T., André, M., Fränz, M., Dubinin, E., … Witasse, O. (2013). Determination of local plasma densities with the MARSIS radar: Asymmetries in the high-altitude Martian ionosphere. *Journal of Geophysical Research: Space Physics*, *118*, 6228–6242. https://doi.org/10.1002/jgra.50593

Andrews, D. J., Edberg, N. J. T., Eriksson, A. I., Gurnett, D. A., Morgan, D., Němec, F., & Opgenoorth, H. J. (2015). Control of the topside Martian ionosphere by crustal magnetic fields. *Journal of Geophysical Research: Space Physics*, *120*, 3042–3058. https://doi.org/10.1002/2014JA020703

Benna, M., Mahaffy, P. R., Grebowsky, J. M., Fox, J. L., Yelle, R. V., & Jakosky, B. M. (2015). First measurements of composition and dynamics of the Martian ionosphere by MAVEN's Neutral Gas and Ion Mass Spectrometer. *Geophysical Research Letters*, *42*, 8958–8965. https://doi.org/10.1002/2015GL066146

Chapman, S. (1931a). The absorption and dissociative or ionizing effect of monochromatic radiation in an atmosphere on a rotating Earth. *Proceedings of the Physical Society*, *43*, 26–45.

Chapman, S. (1931b). The absorption and dissociative or ionizing effect of monochromatic radiation in an atmosphere on a rotating Earth, Part II. Grazing incidence. *Proceedings of the Physical Society*, *43*, 483–501.

Duru, F., Gurnett, D. A., Morgan, D. D., Modolo, R., Nagy, A. F., & Najib, D. (2008). Electron densities in the upper ionosphere of Mars from the excitation of electron plasma oscillations. *Journal of Geophysical Research*, *113*, A07302. https://doi.org/10.1029/2008JA013073

Duru, F., Morgan, D. D., & Gurnett, D. A. (2010). Overlapping ionospheric and surface echoes observed by the Mars Express radar sounder near the Martian terminator. *Geophysical Research Letters*, *37*, L23102. https://doi.org/10.1029/2010GL045859

Duru, F., Gurnett, D. A., Morgan, D. D., Winningham, J. D., Frahm, R. A., & Nagy, A. F. (2011). Nightside ionosphere of Mars studied with local electron densities: A general overview and electron density depressions. *Journal of Geophysical Research*, *116*, A10316. https://doi.org/10.1029/2011JA016835

Ergun, R. E., Morooka, M. W., Andersson, L. A., Fowler, C. M., Delory, G. T., Andrews, D. J., … Jakosky, B. M. (2015). Dayside electron temperature and density profiles at Mars: First results from the MAVEN Langmuir Probe and Waves instrument. *Geophysical Research Letters*, *42*, 8846–8853. https://doi.org/10.1002/2015GL065280

Fowler, C. M., Andersson, L., Halekas, J., Espley, J. R., Mazelle, C., Coughlin, E. R., … Jakosky, B. (2017). Electric and magnetic variations in the near-Mars environment. *Journal of Geophysical Research: Space Physics*, *122*, 8536–8559. https://doi.org/10.1002/2016JA023411

Fox, J. L., & Yeager, K. E. (2006). Morphology of the near-terminator Martian ionosphere: A comparison of models and data. *Journal of Geophysical Research*, *111*, A10309. https://doi.org/10.1029/2006JA011697

Girazian, Z., & Withers, P. (2013). The dependence of peak electron density in the ionosphere of Mars on solar irradiance. *Geophysical Research Letters*, *40*, 1960–1964. https://doi.org/10.1002/grl.50344

Gurnett, D. A., Kirchner, D. L., Huff, R. L., Morgan, D. D., Persoon, A. M., Averkamp, T. F., … Picardi, G. (2005). Radar soundings of the ionosphere of Mars. *Science*, *310*, 1929–1933. https://doi.org/10.1126/science.1121868

Gurnett, D. A., Huff, R. L., Morgan, D. D., Persoon, A. M., Averkamp, T. F., Kirchner, D. L., … Picardi, G. (2008). An overview of radar soundings of the Martian ionosphere from the Mars Express spacecraft. *Advances in Space Research*, *41*, 1335–1346.

Gurnett, D. A., Morgan, D. D., Duru, F., Akalin, F., Winningham, D., Frahm, R. A., … Barabash, S. (2010). Large density fluctuations in the Martian ionosphere as observed by the Mars Express radar sounder. *Icarus*, *206*(1), 83–94. https://doi.org/10.1016/j.icarus.2009.02.019

Jakosky, B. M., Lin, R. P., Grebowsky, J. M., Luhmann, J. G., Mitchell, D. F., Beutelschies, G., … Zurek, R. (2015). The Mars Atmosphere and Volatile Evolution (MAVEN) mission. *Space Science Reviews*, *195*(1), 3–48. https://doi.org/10.1007/s11214-015-0139-x

Jordan, R., Picardi, G., Plaut, J., Wheeler, K., Kirchner, D., Safaeinili, A., … Bombaci, O. (2009). The Mars Express MARSIS sounder instrument. *Space Science Reviews*, *57*, 1975–1986. https://doi.org/10.1016/j.pss.2009.09.016

Kim, E., Seo, H., Kim, J. H., Lee, J. H., Kim, Y. H., Choi, G.-H., & Sim, E.-S. (2012). The analysis of the topside additional layer of Martian ionosphere using MARSIS/Mars Express data. *Journal of Astronomy and Space Sciences*, *29*(4), 337–342. https://doi.org/10.5140/JASS.2012.29.4.337

Kopf, A. J., Gurnett, D. A., Morgan, D. D., & Kirchner, D. K. (2008). Transient layers in the topside ionosphere of Mars. *Geophysical Research Letters*, *35*, L17102. https://doi.org/10.1029/2008GL034948

Mendillo, M., Marusiak, A. G., Withers, P., Morgan, D., & Gurnett, D. (2013). A new semiempirical model of the peak electron density of the Martian ionosphere. *Geophysical Research Letters*, *40*, 1–5. https://doi.org/10.1002/2013GL057631

Morgan, D. D., Gurnett, D. A., Kirchner, D. L., Fox, J. L., Nielsen, E., & Plaut, J. J. (2008). Variation of the Martian ionospheric electron density from Mars Express radar soundings. *Journal of Geophysical Research*, *113*, A09303. https://doi.org/10.1029/2008JA013313

Morgan, D. D., Witasse, O., Nielsen, E., Gurnett, D. A., Duru, F., & Kirchner, D. L. (2013). The processing of electron density profiles from the Mars Express MARSIS topside sounder. *Radio Science*, *48*, 197–207. https://doi.org/10.1002/rds.20023

Němec, F., Morgan, D. D., Gurnett, D. A., & Duru, F. (2010). Nightside ionosphere of Mars: Radar soundings by the Mars Express spacecraft. *Journal of Geophysical Research*, *115*, E12009. https://doi.org/10.1029/2010JE003663

Němec, F., Morgan, D. D., Gurnett, D. A., Duru, F., & Truhlík, V. (2011). Dayside ionosphere of Mars: Empirical model based on data from the MARSIS instrument. *Journal of Geophysical Research*, *116*, E07003. https://doi.org/10.1029/2010JE003789

Němec, F., Morgan, D. D., Gurnett, D. A., & Andrews, D. J. (2016). Empirical model of the Martian dayside ionosphere: Effects of crustal magnetic fields and solar ionizing flux at higher altitudes. *Journal of Geophysical Research: Space Physics*, *121*, 1760–1771. https://doi.org/10.1002/2015JA022060

Němec, F., Morgan, D. D., & Gurnett, D. A. (2016). On improving the accuracy of electron density profiles obtained at high altitudes by the ionospheric sounder on the Mars Express spacecraft. *Journal of Geophysical Research: Space Physics*, *121*, 10,117–10,129. https://doi.org/10.1002/2016JA023054

Picardi, G., Biccari, D., Seu, R., Plaut, J., Johnson, W. T. K., Safaeinili, R. L. J. A., … Zampolini, E. (2004). MARSIS: Mars advanced radar for subsurface and ionosphere sounding. In Wilson, A., & Chicarro, A. (Eds.), *Mars Express: The Scientific Payload* (Vol. 1240, pp. 51–69). Noordwijk: ESA Special Publication.

Sánchez-Cano, B., Radicella, S. M., Herraiz, M., Witasse, O., & Rodríguez-Caderot, G. (2013). NeMars: An empirical model of the Martian dayside ionosphere based on Mars Express MARSIS data. *Icarus*, *225*, 236–247. https://doi.org/10.1016/j.icarus.2013.03.021

Vogt, M. F., Withers, P., Fallows, K., Flynn, C. L., Andrews, D. J., Duru, F., & Morgan, D. D. (2016). Electron densities in the ionosphere of Mars: A comparison of MARSIS and radio occultation measurements. *Journal of Geophysical Research: Space Physics*, *121*, 10,241–10,257. https://doi.org/10.1002/2016JA022987

Wang, X.-D., Wang, J.-S., & Zou, H. (2012). On the small-scale fluctuations in the peak electron density of Martian ionosphere observed by MEX/MARSIS. *Planetary and Space Science*, *63–64*, 87–93. https://doi.org/10.1016/j.pss.2011.10.007

Withers, P. (2009). A review of observed variability in the dayside ionosphere of Mars. *Advances in Space Research*, *44*, 277–3078. https://doi.org/10.1016/j.asr.2009.04.027

Withers, P., Fallows, K., Girazian, Z., Matta, M., Häusler, B., Hinson, D., … Witasse, O. (2012). A clear view of multifaceted dayside ionosphere of Mars. *Geophysical Research Letters*, *39*, L18202. https://doi.org/10.1029/2012GL053193

Withers, P., Fillingim, M. O., Lillis, R. J., Häusler, B., Hinson, D. P., Tyler, G. L., … Witasse, O. (2012). Observations of the night-side ionosphere of Mars by the Mars Express Radio Science Experiment (MaRS). *Journal of Geophysical Research*, *117*, A12307. https://doi.org/10.1029/2012JA018185